Proceeding of ICNM - 2009

****

Synthesis and Characterization of Gd and Sb Doped SnO$_2$ Conductive Nanoparticles

Liu Xiaozhen[1*]，Chen Jie[2]，Wu Yan[1], Xu Jie[1]

(1. Department of Chemical Engineering, Shanghai Institute of Technology, Shanghai 200235, China;
2. Department of Chemistry, Georgetown University, Washington, 20057-1013, USA)

Abstract: Gd was used as a dopant for the first time in preparing conductive powder to improve its performance. Gd and Sb doped SnO$_2$ conductive nanoparticles were prepared by the complexation-coprecipitation method with Sn, Sb$_2$O$_3$ and Gd$_2$O$_3$ as the raw materials. Thermal behavior, crystal phase, and structure of the prepared conductive nanoparticles were characterized by TG/DSC, FTIR, XRD and TEM techniques, respectively. The resistivity of the prepared conductive nanoparticles is 0.29Ωcm; TG/DSC curves show that the precursors lose weight completely before 750 ; FTIR spectrum shows that the vibration peak are wide peak in 711 cm^{-1} -600cm^{-1}; the Gd and Sb doped SnO$_2$ conductive nanoparticles have intense absorption in 4000 cm^{-1}- 1600 cm^{-1}; Gd and Sb doped SnO$_2$ have a structure of tetragonal rutile; complex doping is achieved well by complexation-coprecipitation method and is recognized as replacement doping or caulking doping; TME shows that the particles were weakly agglomerated, the size of the particles calcined at 800 ranged approximately from 10 to 30 nm.

Key words: conductive nanoparticles; doping; chemical synthesis; spectra; rare earths
CLC number: O434.19, O657.33 **Document code:** A **Article ID:**

Sb doped SnO$_2$ was a semiconductor. At doping levels of about 2 % to 7 % antimony, metallic properties were displayed [1]. The powder of antimony doped tin oxide has been widely used in photovoltaic and optoelectronic devices, flat panel displays, electrochromic materials and electrode materials for their electric and optical advantage properties [2-6]. It is generally accepted that paint coatings could represent a much cheaper alternative for spectrally selective solar collector surfaces, and also as lowemittance coatings in window glazing. Besides a resin binder, such the paint should contain a conductive pigment and would also exhibit antistatic properties. So far, antistatic coatings havebeen confined mainly to carbon blacks and metallic pigments. Moreover, organic polymer binders were mostly cationic electrolytes and therefore sensitive to humidity and not suitable for exposure to external conditions[2]. Antimony- tin oxide catalysts are well known to be active and selective for olefin oxidation, oxidative dehydrogenation, and ammoxidation of alkenes, notably propylene to acrolein and acrylonitrile, and have previously been developed for the selective oxidation of hydrocarbons [7]. The use temperature of the conductive powders is raised by rare earths being doped in antimony-tin oxide [8-9]. Across the world, unredeemable metallic resources are scarcer than ever before. Nonmetallic resources, such as quartz, which have rich abundance and low prices, are desirable to be exploited.

Generally, antimony doped tin oxide powder are prepared by a coprecipitation method with SnCl$_4$and SbCl$_3$ as the raw materials [10-11]. It is well known that chlorine ions adsorbed on tin hydroxide are very difficult to be rinsed

off. The existence of Cl$^-$ produced harmful effect to the conductivity and produced serious corrosion to electronic components in the course of the application. Furthermore, the optimally calcining temperature of antimony doped tin oxide conductive nanoparticles prepared by coprecipitation method is 600 [12].

In this paper, Gd was used as a dopant for the first time in preparing conductive powder to improve its performance, Gd and Sb doped SnO_2 conductive nanoparticles were prepared by the complexation-coprecipitation method with Sn, Sb_2O_3 and Gd_2O_3 as the raw materials. The preparative method is simple and easy to manufacture on large scale. The properties of the nanoparticles were studied with TG/DSC, FTIR, X-ray diffraction and TEM.

1 Experimental

1.1 Preparation of conductive nanoparticles

Gd and Sb doped SnO_2 conductive nanoparticles were prepared by the complexation-coprecipitation using the following procedure. Weighed amount of Gd_2O_3 (purity>99.999%) was dissolved in nitric acid. The liquid was removed to a volumetric flask, diluted with 18.3 MΩ·cm water to graduation. Weighed amounts of Sn powder [analytical reagent grade (AR)], Sb_2O_3 (AR) and citric acid (AR) with suitable molar ratios were added to a flask and stirred. 3 mol/L HNO_3 was added dropwise slowly until a light green transparent solution was formed. An amount of $Gd(NO_3)_3$ solution (mentioned above) was added into the light green solution and the mixture solution was formed. The mixture solution was added dropwise to 6 mol/L $NH_3 \cdot H_2O$ solution until pH of solution reached 8.5-9.0. The precipitate was collected by centrifugation and washed with 18.3 MΩ·cm water and ethanol two times respectively. The precursors were dried at 100℃ for 3h, ground and were afterwards calcined for 1h at specific temperature in the range of 600-800℃. According to procedure above, samples of Gd and Sb doped SnO_2 conductive nanoparticles with molar ratios $n(Sb_2O_3):n(Sn):n(Gd_2O_3)$= 1:25:0.0125, 1:25:0.025, 1:25:0.05, 1:25:0.10, 1:25:0.15, 1:25:0.20,and 1:25:0.25 were synthesized, respectively. The precursors were calcined at 800℃ for 1h. Moreover, samples of Sb doped SnO_2 conductive nanoparticles with molar ratios $n(Sb_2O_3):n(Sn)$ were 1:10, 1:15, 1:20, 1:25, 1:30 and 1:35, were also prepared respectively as control. The precursors were calcined at 600℃ for 5h. Furthermore，the sample of SnO_2 was also prepared as control. The precursors were calcined at 800℃ for 5h.

1.2 Characterization techniques

1.2.1 Surface resistivity measurement

Weigh a specific amount of synthesized samples of conductive nanoparticles. The nanoparticles were putted into Φ =1.3mm model of stainless steel, pressed into slice with 20MPa pressure. Surface resistivity measurement was performed on an ordinary SX1934 four-point measurement devise.

1.2.2 XRD measurement

X-ray powder diffraction patterns of the synthesized samples were acquired with a Rigaku D/max 2550 VB/PC X-ray diffractometer, using Cu Kα radiation. A continuous scan mode was used to collect 2θ data from 20-80° with a 0.02 sampling pitch and a 2° min^{-1} scan rate. X-ray tube voltage and current were set at 40 kV and 30 mA, respectively. The samples were synthesized SnO_2 nanoparticles, Sb doped SnO_2 conductive nanoparticles [$n(Sb_2O_3):n(Sn)$ =1:25]and Gd and Sb doped SnO_2 conductive nanoparticles [$n(Sb_2O_3):n(Sn):n(Gd_2O_3)$= 1:25:0.05], respectively.

1.2.3 Thermal analysis

Thermogravimetry (TG) and differential scanning calorimetry (DSC) were carried out with a Netzschsta STA449C Thermo-gravimetric analyzer.18.004 mg of the precursors dried at 100℃ were placed in a sample holder and were heated from 52℃ to 1000℃ with a rate of 10℃/ min in air, while weight change and

endothermic change were recorded as function of temperature.

1.2.4 FTIR measurement

Infrared absorption spectra of the precursors dried at 100°C and calcined at 800°C with molar ratio $n(Sb_2O_3):n(Sn):n(Gd_2O_3)= 1:25:0.05$ were determined by a Avatar 360 FTIR infrared spectrophotometer by potassium bromide disc method respectively.

1.2.5 TEM measurement

The morphology of Gd and Sb doped SnO_2 conductive nanoparticles[$n(Sb_2O_3):n(Sn):n(Gd_2O_3)= 1:25:0.05$] was made with a JEM-200CX transmission electron microcopey (TEM).

2   Results and discussion :

2.1 Influences of quantity of dopants to the resistivities of the conductive nanoparticles

Table 1. Influences of quantity of Sb to the resistivities of Sb doped SnO$_2$ conductive nanoparticles

$n(Sb_2O_3):n(Sn)$	1:10	1:15	1:20	1:25	1:30	1:35
$\rho/\Omega\cdot cm$	6.12	1.44	0.90	0.41	0.74	0.88

Table 2. Influences of quantity of Gd to the resistivities of Gd and Sb doped SnO$_2$ conductive nanoparticles

$n(Sb_2O_3):n(Sn):n(Gd_2O_3)$	1:25:0.015	1:25:0.025	1:25:0.05	1:25:0.10	1:25:0.15
$\rho/\Omega\cdot cm$	0.70	0.61	0.28	0.62	0.79

Table 1 shows the influences of quantity of Sb to the resistivities of Sb doped SnO_2 conductive nanoparticles. Table 2 show the influences of quantity of Gd to the resistivities of Gd and Sb doped SnO_2 conductive nanoparticles. According to Table1, when the molar ratios $n(Sb_2O_3):n(Sn)$ are in the range of 1:10-1:35, the resistivity of Sb doped SnO_2 conductive nanoparticles reduces at first with the decrease of the molar ratio $n(Sb_2O_3):n(Sn)$ until it reaches minimum with a value of 0.41Ω when the molar ratio $n(Sb_2O_3):n(Sn)=1:25$. Then the resistivity increases when the molar ratio $n(Sb_2O_3):n(Sn)$ decreases continuously. According to Table 2, when molar ratio $n(Sb_2O_3):n(Sn)$ is 1:25, molar ratio $n(Sb_2O_3):n(Sn):n(Gd_2O_3)$ are in the range of 1:25:0.015- 1:25:0.15, the resistivity of Gd and Sb doped SnO_2 conductive nanoparticles decreases when the quantity of doping Gd increases at the beginning. The resistivity has a minimum of 0.28Ω·cm when the molar ratio $n(Sb_2O_3):n(Sn):n(Gd_2O_3)$ =1:25:0.05. Then the resistivity increases when the quantity of doping Gd increases continuously.

The optimally calcining temperature of antimony doped tin oxide conductive nanoparticles is 600 [2]. The resistivity of Sb doped SnO_2 conductive particles reaches minimum with a value of 0.41Ω when the molar ratio $n(Sb_2O_3):n(Sn)=1:25$. The resistivity of Gd and Sb doped SnO_2 has a minimum of 0.29Ω·cm when the molar ratio $n(Sb_2O_3):n(Sn):n(Gd_2O_3)$ =1:25:0.025. The calcining temperature of Gd and Sb doped SnO_2 is 800 . The optimally applicable temperature of Gd and Sb doped SnO_2 is 200 higher than optimally applicable temperature of Sb doped SnO_2. What is more, the resistivity of Gd and Sb doped SnO_2 is smaller than that of Sb doped SnO_2.
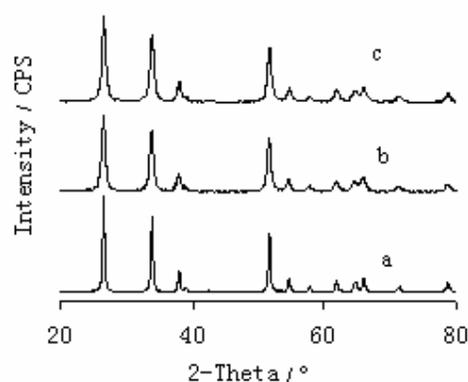
2.2 XRD studies

Figure 1. XRD spectra of SnO_2 nanoparticles , Sb doped SnO_2 conductive nanoparticles [n(Sb_2O_3):n(Sn)=1:25]and
Gd and Sb doped SnO_2 conductive nanoparticles [n(Sb_2O_3):n(Sn):n(Gd_2O_3)=1:25:0.025]

a- SnO_2;   b- Sb doped SnO_2;   c- Gd and Sb doped SnO_2

Figure 1 shows XRD spectra of SnO_2 nanoparticles, Sb doped SnO_2 conductive nanoparticles and Gd and Sb doped SnO_2 conductive nanoparticles respectively. According to Figure 1, the diffraction peaks in the XRD spectra of Sb doped SnO_2 conductive nanoparticles and Gd and Sb doped SnO_2 conductive nanoparticles can be recognized as the characteristic ones of SnO_2, which demonstrates that the samples have a structure of tetragonal rutile. Moreover, they give the diffraction peaks a small migration, which demonstrates that the complex doping can be achieved better by complexation-coprecipitation method and be recognized as replacement doping or caulking doping.

Table 3. Diffraction peaks 2θ of SnO_2, Sb doped SnO_2 and Gd and Sb doped SnO_2 nanoparticles

(hkl)	(110)	(101)	(200)	(111)	(210)	(211)	(220)	(002)	(310)	(112)	(301)	(202)	(321)
SnO_2	26.56	33.84	37.92	38.92	42.64	51.76	54.80	57.84	61.88	64.72	65.92	71.32	78.72
Sb-SnO_2	26.52	33.80	37.92	38.84	42.68	51.80	54.60	57.80	61.88	64.68	65.85	71.24	78.72
Gd-Sb-SnO_2	26.52	33.76	37.84	38.88	42.60	51.84	54.64	57.68	61.96	64.64	65.80	71.16	78.72

According to Table 3, with the doping of Gd into Sb-SnO_2, the diffraction angles 2θ of peaks (200), (002) and (202) have a large variation respectively, demonstrating Gd's replacement in the SnO_2 lattice. The diffraction angle 2θ of peak (110) remains the same with the doping of Gd into Sb-SnO_2, which proves that the doping of Sb in the Gd and Sb conductive nanoparticles can be recognized as replacement doping or caulking doping.

2.3 Thermal analysis
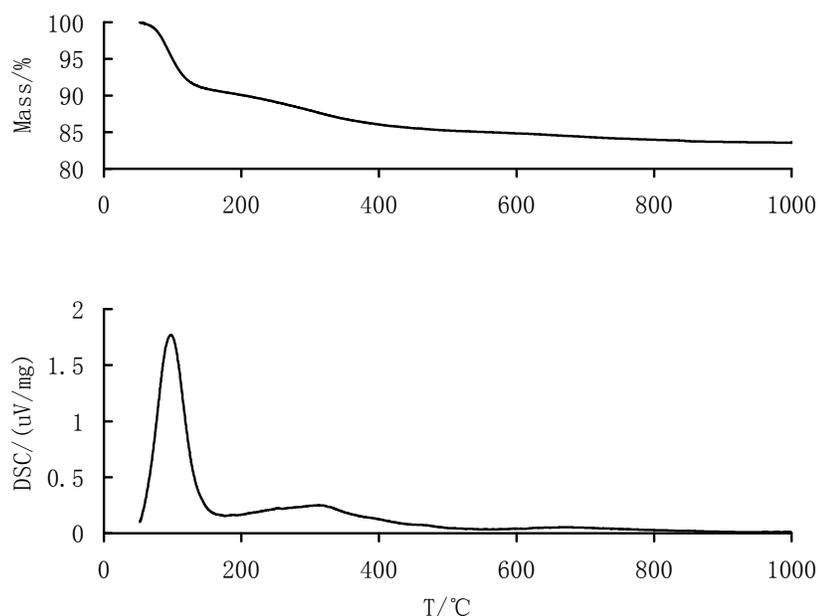

Fig.2. TG and DSC curves of the precursors dried at 100℃

TG and DSC as shown in Fig. 2 recorded the history of pyrolytic process of the precursors drying at 100℃. As can be seen, the TG curve shows a two-stage weight loss profile, the weight loss is 16.44%. The first stage, a fast weight loss stage claimed 9.98% in the range of 52-200 ℃, are attributed to the loss of water, since the precursors easily absorbs water, corresponding to the high endothermic peaks at 102.5 ℃ in DSC curve. The second weight loss stage claimed 5.98% in the range of 200-750 ℃, is attributed to the pyrolysis of NO_3^- [12] and the loss of water, is due to the precursors absorbs a small amount of NO_3^- and change the precursors (SnO_3H_2) into SnO_2 [12], corresponding to the high endothermic peaks at 317.4 ℃ in DSC curve. After 750 ℃, the TG curve is a horizontal line, shows loss of water essential finish.

2.4 Infrared spectra

Figure 3-4 show FTIR spectra of Gd and Sb doped SnO_2 with a molar ratio $n(Sb_2O_3):n(Sn):n(Gd_2O_3)= 1:25:0.025$ and the samples were dried at 100℃ and calcined at 800℃, respectively. According to Figure 3, there are a Sn-OH vibration peak at 560cm^{-1}[13-14], $Gd(NO_3)_3$ vibration peaks at 650cm^{-1}, 1380cm^{-1} and 1630cm^{-1}[15], NO_3^- vibration peaks at 1384cm^{-1} and 1637cm^{-1}[16] and a –OH vibration peak of water at 3124cm^{-1}, which demonstrates that a small amount of adsorbed water and NO_3^- ions existing in the nanoparticles. According to Figure 4, Sn-OH vibration peak at 560cm^{-1} almost disappears after calcination at 800℃. However, there is a newly forming Sn-O stretching vibration peak at 620cm^{-1}, which demonstrates that the precursors might be completely desiccated and changed into oxides of tin. Sb doped SnO_2 nanoparticles have a sharp peak at about 630cm^{-1}[17] Gd and Sb doped SnO_2 nanoparticles have a broad absorption peak in the range of 711cm^{-1}-600cm^{-1} for v_{Gd-O} has characterized absorption peaks in the range of 600cm^{-1}[18]. NO_3^- peaks at 1384cm^{-1} and 1637cm^{-1} and –OH vibration peak of water at 3124cm^{-1} existing in Figure 4 completely disappear, which demonstrates that the nitrate ions and water have been completely evaporated. Gd and Sb doped nanoparticles have strong absorption in the range of 4000cm^{-1}-1600cm^{-1}.
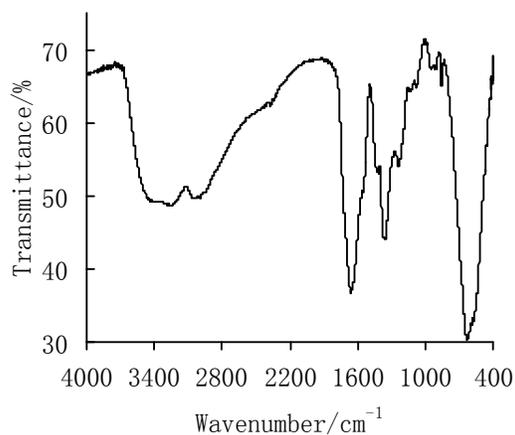
Fig. 3 FTIR spectrum of Gd and Sb doped SnO_2 conductive nanoparticles [$n(Sb_2O_3)$:$n(Sn)$:$n(Gd_2O_3)$ =1:25:0.025] dried at 100℃
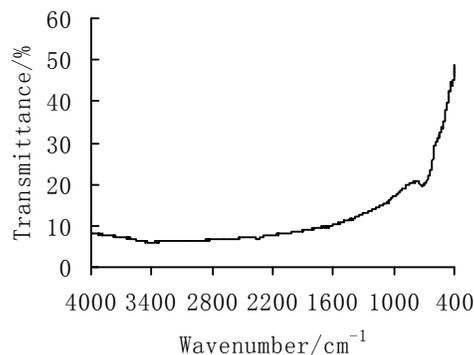
Fig. 4 FTIR spectrum of Gd and Sb doped SnO_2 conductive nanoparticles [$n(Sb_2O_3)$:$n(Sn)$:$n(Gd_2O_3)$ =1:25:0.025] calcined at 800℃
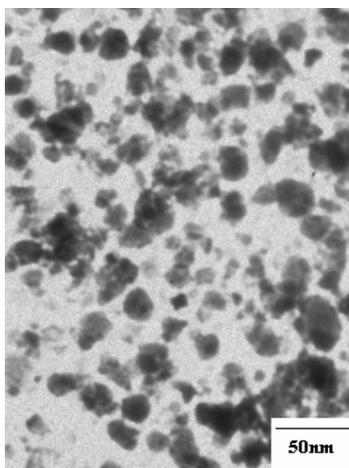
2.5 TEM image

Fig. 5 TEM image of Gd and Sb doped SnO_2 conductive nanoparticles calcined at 800℃

Figure 5 shows TEM image of Gd and Sb doped SnO_2 conductive nanoparticles calcined at 800℃. The diameter of particles is about 10-30 nm. Conductive particles prepared by complexation-coprecipitation method are of nano-scale. The dispersibility of nanoparticles prepared by complexation-coprecipitation method is well. The coordination characteristic of citric acid makes the coprecipitation process more evenly and reduces the agglomeration of particles.

3. Conclusions

Gd and Sb doped SnO_2 conductive nanoparticles are synthesized by the complexation-coprecipitation method with Sn, Sb_2O_3, Gd_2O_3 and citric acid as raw materials. The particle diameter and resistivity of synthesized conductive nanoparticles are 10-30 nm and 0.29 Ω·cm, respectively. TG/DSC curves show that the precursors lose weight completely before 750 ℃. FTIR spectrum shows that the vibration peak is wide peak in 711cm^{-1}-600cm^{-1}, the Gd and Sb doped SnO_2 conductive nanoparticles have intense absorption in 4000 cm^{-1}-1600 cm^{-1}. Complex doping is achieved well by complexation-coprecipitation method and is recognized as

replacement doping or caulking doping.

References

[1] Rockenberger J, Zumfelde U, Tischer M. Near edge X-ray absorption fine structure measurements (XANES) and extended X-ray absorption fine structure measurements (EXAFS) of the valence state and coordination of antimony in doped nanocrystalline SnO_2[J]. J. Chem. Phys., 2000, 112: 4296.

[2] Crnjakorel Z, Orel B, Conductive SnO_2 / Sb powder: preparation and optical properties. J. Mater. Sci., 1992, 27: 313.

[3] Zhang Jianrong, Gao Lian. Hydrothermal synthesis and characterization of SnO_2 nanoparticles, Acta Chim. Sinica. 2003, 61:1965.

[4] Zhang Jianrong, Gao Lian. Crystal and electrical behaviour of antimony doped SnO_2 nanoparticles. Chinese Journal of Applied Chemstry, 2002, 19: 552.

[5] Rembeza E S, Richard O, Van Landuyt J.Influence of laser and isothermal treatments on microstructural properties of SnO_2 films. Materials Research Bulletin, 1999, 34: 1527.

[6] Guglielmi M, Menegazzo E, Gasparro G, et al. Journal of Sol-Gel Science and Technology, 1998, 13: 679.

[7] Vincent Dusastre and David E. Williams. Sb(III) as a surface site for water adsorption on $Sn(Sb)O_2$, and its effect on catalytic activity and sensor behavior [J]. J. Phys. Chem. B, 1998, 102: 6732.

[8] Liu Xiaozhen, Preparation of Sb and rare earths doped SnO_2 conductive powder [P]. CN 200410053276.2, 2004.

[9] Liu Xiaozhen, Preparation of Sb and rare earths doped SnO_2 compound conductive powder [P].CN 200410053277.7, 2004.

[10] Bose AC, Kalpana D, Thangadurai P, Ramasamy S. Synthesis and characterization of nanocrystalline SnO_2 and fabrication of lithium using nano- SnO_2 [J]. J. Power Source, 2002, 107, 138.

[11] Koivula R, Hajula R, Lehto J. Structure and ion exchange properties of tin antimonates with various Sn and Sb contents [J]. Mesopor. Mater, 2002, 55, 231.

[12] Zhang, J. R.; Gao, L. Synthesis and characterization of antimony-doped tin oxide (ATO) nanoparticles [J]. Inorg. Chem. Commun., 2004, 7: 91.

[12] Zhang Jianrong, Gao Lian. Hydrothermal synthesis and characterization of SnO_2 nanoparticles [J]. Acta Chim. Sinica. 2003, 61:1965.

[13] Senguttuvan T D, Malhotra L K. Sol gel deposition of pure and antimony doped tin dioxide thin films by non alkoxide precursors [J].Thin Solid Films 1996, 289: 22.

[14 Lin YJ, Wu C. The properties of antimony-doped tin oxide thin films from the sol-gel process [J]. J. Surf. Coat. Tech., 1997, 88: 23.

[15] Sadtler Research Laboratories. Inorganics IR Grating Spectra. 1973, 3-5: Y1151K.

[16] Zhang, J. R.; Gao, L. J. Synthesis and characterization of nanocrystalline tin oxide by sol–gel method [J]. Solid State Chem. 2004, 177, 1425.

[17] Crnjakorel Z, Orel B. Conductive SnO_2 / Sb powder: preparation and optical properties [J]. J. Mater. Sci. 1992, 27, 313.

[18] Sadtler Research Laboratories. Inorganics IR Grating Spectra. 1973, 3-5: Y749K.